Science Arts & Métiers (SAM)

is an open access repository that collects the work of Arts et Métiers Institute of Technology researchers and makes it freely available over the web where possible.

This is an author-deposited version published in: https://sam.ensam.eu
Handle ID: .http://hdl.handle.net/10985/8922

To cite this version :

Ali KOMATY, Abdel-Ouahab BOUDRAA, Benoit AUGIER, Delphine DARE-EMZIVAT - EMD-Based Filtering Using Similarity Measure Between Probability Density Functions of IMFs - IEEE Transactions on Instrumentation and Measurement - Vol. 63, n°1, p.27-34 - 2014

Any correspondence concerning this service should be sent to the repository Administrator : scienceouverte@ensam.eu

Arts et Métiers Institute of Technology

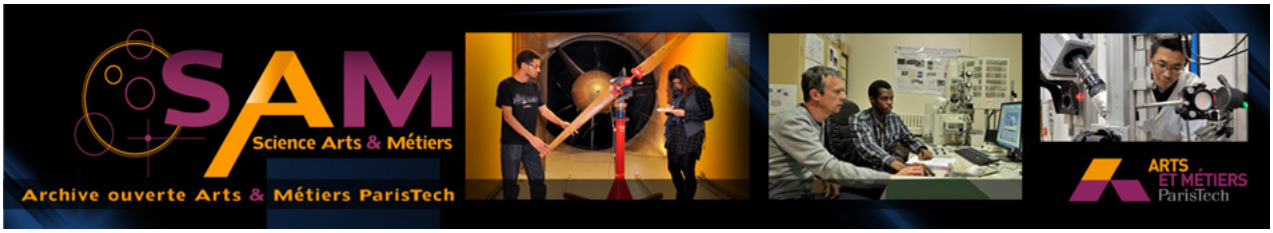

Science Arts & Métiers (SAM)

is an open access repository that collects the work of Arts et Métiers ParisTech researchers and makes it freely available over the web where possible.

This is an author-deposited version published in: http://sam.ensam.eu
Handle ID: .http://hdl.handle.net/10985/8922

To cite this version :

Ali KOMATY, Abdel-ouahab BOUDRAA, Benoit AUGIER, Delphine DARE - EMD-Based Filtering Using Similarity Measure Between Probability Density Functions of IMFs - IEEE TRANSACTIONS ON INSTRUMENTATION AND MEASUREMENT - Vol. 63, n°1, p.27-34 - 2014

Any correspondence concerning this service should be sent to the repository
Administrator : archiveouverte@ensam.eu

EMD-Based Filtering Using Similarity Measure Between Probability Density Functions of IMFs

Ali Komaty, *Student Member, IEEE*, Abdel-Ouahab Boudraa, *Senior Member, IEEE*, Benoit Augier, and Delphine Daré-Emzivat

***Abstract*— This paper introduces a new signal-filtering, which combines the empirical mode decomposition (EMD) and a similarity measure. A noisy signal is adaptively broken down into oscillatory components called intrinsic mode functions by EMD followed by an estimation of the probability density function (pdf) of each extracted mode. The key idea of this paper is to make use of partial reconstruction, the relevant modes being selected on the basis of a striking similarity between the pdf of the input signal and that of each mode. Different similarity measures are investigated and compared. The obtained results, on simulated and real signals, show the effectiveness of the pdf-based filtering strategy for removing both white Gaussian and colored noises and demonstrate its superior performance over partial reconstruction approaches reported in the literature.**

***Index Terms*— Consecutive mean squared error (CMSE), empirical mode decomposition (EMD), intrinsic mode function (IMF), probability density function (pdf), signal filtering, similarity measure.**

I. Introduction

NOISE is a major challenge in many measurement processes such as partial discharge measurement [1], frequency estimation of three-phase power system [2], or dielectric response measurements of transformer insulation [3]. Noise removal is an important topic in instrumentation and measurement domains where the challenge is to preserve the important structures of the signals while removing the noise [1]–[4]. Efficient and robust denoising strategy aims at reducing uncertainties of the observed data [5] and improve their quality. A variety of noise reduction methods have been developed mostly based on the model-based methods, transform domain approaches, and adaptive filtering. Linear methods such as Wiener filter are largely used because they are easy to implement and to design. Such methods, however, rely on the critical assumption of stationary signals. To overcome this limit, nonlinear methods have been proposed and especially those based on wavelet thresholding [6]. But a limit of the wavelet approach is that the basic functions are fixed, and thus do not necessarily match all real signals. More precisely, a difficulty of this analysis is its nonadaptive nature. Once, the basic wavelet is selected, one will have to use it for analyzing all the data [7]. Using inappropriate wavelet decomposition will limit the performance of the wavelet-based signals denoising scheme. Recently, empirical mode decomposition (EMD), has been introduced for analyzing the data from nonstationary and nonlinear processes [7]. This expansion decomposes adaptively any signal into oscillatory components called intrinsic mode functions (IMFs). Thus, this powerful adaptive tool is well suited to solve problems such as noise or frequency estimation in measurements domains. It has been shown that based on partial reconstruction of relevant modes, EMD performs signals filtering in an adaptive way [8]. However, it still raises the question on how to select such modes in an efficient way. When EMD is applied to a noisy data, physical interpretation of the extracted modes is necessary to determine, which IMFs are pure noise, pure signal, or contains both. A statistical significance of IMFs by studying the statistical characteristics of uniformly distributed white noise is revealed in [9]. Using these characteristics, each mode is classified based on its energy-density spread function. References [10] and [11] use a correlation-based threshold to discriminate between relevant and irrelevant IMFs. For very noisy signals, both of these methods perform poorly mainly because of the strong correlation between the noisy signal and the first modes. Such approaches require setting an appropriate threshold for discriminating between relevant and irrelevant IMFs. An analogue approach based on consecutive mean squared error (CMSE) criterion has been proposed in [8] where the signal is reconstructed from the mode, for which this criterion is minimal. The CMSE selects the IMF order where the first significant change in energy occurs. This approach works satisfactory in most of the cases and without the use of a threshold, but in some cases CMSE criterion can be trapped in a local minima. To avoid these shortcomings, in this paper a more robust filtering scheme is presented. This filtering makes use of partial reconstruction, the relevant modes being selected on the basis of similarity between the probability density function (pdf) of the input signal and that of each mode. Higher values of this similarity indicate that the compared signals possess similar characteristics, and thus the associated modes should be included in the reconstructed signal. Our preliminary results show that probabilistic similarity, based on Hausdorff distance (HD), is more robust against noise that the correlation-based approach [11] and reveals better the underlying structures of the signal [12].

The outline of this paper is as follows. Description of the EMD is given in Section II followed by the filtering strategy

Manuscript received February 2, 2013; revised April 29, 2013; accepted April 30, 2013. Date of publication August 19, 2013; date of current version December 5, 2013. The Associate Editor coordinating the review process was Dr. Kurt Barbe.

The authors are with Ecole Navale, IRENav, BREST Cedex 9 29240, France (e-mail: ali.komaty@ecole-navale.fr; boudra@ecole-navale.fr; augier.ben@gmail.com; delphine.dare@ecole-navale.fr).

Color versions of one or more of the figures in this paper are available online at http://ieeexplore.ieee.org.

Digital Object Identifier 10.1109/TIM.2013.2275243

is Section III. Results on simulated and real data are presented and discussed in Section III. Finally, Section IV concludes this paper with a summary and some directions for future research.

II. Filtering Strategy

The EMD decomposes any signal $x(t)$ into a set of IMFs each one with a distinct time scale [7]. The decomposition is based on the local time scale of $x(t)$, and yields adaptive basis functions. It results that $x(t)$ is expressed as

$$x(t) = \sum_{j=1}^{C} \mathrm{IMF}_j(t) + r_C(t) \tag{1}$$

where $\mathrm{IMF}_j(t)$ is the IMF of order j, $\mathrm{r}_C(t)$ is the residual, and C is the number of IMFs. The extracted modes are almost orthogonal and they form a complete set by the virtue of the fact that summing all these modes with the residue recovers $x(t)$, within machine precision. A striking property of the EMD is its ability to act as a filter. The advantage of such filtering is that the results preserve nonlinearity, nonstationarity, and full meaning in physical space. The use of EMD as a filter is essentially a partial reconstruction process of relevant modes [8]. These modes are selected based on a given criterion that identifies the modes carrying information relevant to underlying main structures of the input signal. Consider a noise-free signal $y(t)$ contaminated by an additive noise $n(t)$

$$x(t) = y(t) + n(t). \tag{2}$$

The aim is to find an estimate $\tilde{y}(t)$ of $y(t)$ from $x(t)$

$$\tilde{y}(t) = \sum_{i=k_{\mathrm{th}}}^{C} \mathrm{IMF}_i(t) + r_C(t) \tag{3}$$

where kth is index of the partial reconstruction. The open question for using (3) as a filter is how to choose the order kth. The novelty of the proposed method is to tackle this problem by taking advantage of the IMFs statistics combined with a robust similarity measure. Because an important property of a signal is its oscillation amplitude, we exploit the pdf, function of amplitude, of each mode. Based on Bayesian interpretation, a pdf represents a state of knowledge about the systems or signals of interest rather than merely a frequency. Because a pdf contains a complete information about its corresponding IMF, one can expect a pdf similarity measure to identify the IMFs dominantly catching the features of $y(t)$. Hereafter, we will be using the normal Kernel density function to estimate mode's pdf. One way to discriminate between relevant and irrelevant IMFs is to compare their pdfs using a similarity measure. The aim is to seek such measure that identifies the modes capturing the underlying structures of $y(t)$. In the following, we review some well-known measures and emphasize some of their characteristics. This review includes the HD recently used by the authors to compare the pdfs of pair of 1-D signals [12].

A. Review of Some Similarity Measures

Similarity measures can be classified into two categories: 1) the information-theoretic measures such as Kullback–Leibler divergence (KLD) and 2) that is based on metrics such as HD, which are sensitive to the geometry (e.g., area,. . .) and measure how far two subsets of a metric space are from each other.

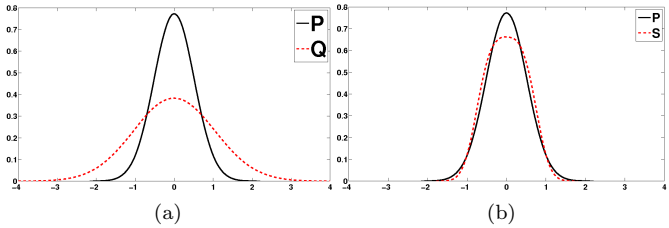

(a) (b)

Fig. 1. Shape of the distribution affects the KLD more than the geometrical distance. (a) Distributions $\mathrm{P} = \mathrm{pdf}(\mathcal{N}(0,\sigma_1))$ and $\mathrm{Q} = \mathrm{pdf}(\mathcal{N}(0,\sigma_2))$. (b) Distributions $\mathrm{P} = \mathrm{pdf}(\mathcal{N}(0,\sigma_1))$ and $\mathrm{S} = \mathrm{pdf}\{\mathcal{N}(0,\sigma_3) + \mathcal{U}(-a,a)\}$.

TABLE I
Information-Theoretic Measures Calculated for the Densities Shown in Fig. 1

	Fig. 1(a)	Fig. 1(b)	
Methods	d(P,Q)	d(P,S)	Δ
KLD	1.725×10^{-4}	0.0516	-0.0514
KLD_{sym}	1.742×10^{-4}	0.0538	-0.0536
JSD	4.838×10^{-5}	0.0134	-0.0133

B. Information Theoretic Measures

KLD is the most frequently used information-theoretic distance measure and is defined as follows:

$$\mathrm{KLD(P||Q)} := \int_{-\infty}^{+\infty} \mathrm{P(z)} \log \frac{\mathrm{P(z)}}{\mathrm{Q(z)}} \mathrm{dz} \tag{4}$$

where P and Q are two pdfs. A symmetric version of KLD ($\mathrm{KLD_{sym}}$) is defined as follows [13]:

$$\mathrm{KLD_{sym}(P||Q)} := \frac{\mathrm{KLD(P||Q)} + \mathrm{KLD(Q||P)}}{2}. \tag{5}$$

Another measure is the Jensen–Shannon divergence (JSD). It is a symmetrized and smoothed version of the KLD, which has always finite values. JSD is defined by

$$\mathrm{JSD(P||Q)} := \frac{\mathrm{KLD(P||M)} + \mathrm{KLD(Q||M)}}{2} \tag{6}$$

where $\mathrm{M} = 1/2(\mathrm{P} + \mathrm{Q})$. Even if these measures have acceptable geometric properties [13], they are very sensitive to the distribution shape. We show this effect in Fig. 1 where two pdfs are compared. Fig. 1(a) shows the two distributions $\mathrm{P} = \mathrm{pdf}(\mathcal{N}(0,\sigma_1))$ and $\mathrm{Q} = \mathrm{pdf}(\mathcal{N}(0,\sigma_2))$. Fig. 1(b) shows the same distribution P compared with the distribution $\mathrm{S} = \mathrm{pdf}\{\mathcal{N}(0,\sigma_3) + \mathcal{U}(-\mathrm{a},\mathrm{a})\}$ where $\mathcal{U}(-a,a)$ is a uniform distribution defined on interval $[-a,a]$. Table I shows the results of the three information-theoretic measures applied to distributions of Fig. 1. We note by d(P, Q) and d(P, S) the distances between the pdfs shown in Fig. 1(a) and (b) and their difference is noted by $\Delta = \mathrm{d(P,Q)} - \mathrm{d(P,S)}$. If $\Delta < 0$, this means that Q is closer to P than S. Although the large geometric distance between P and Q, the corresponding information-theoretic measures give very small values compared with the

TABLE II

DISTANCES OF DENSITIES SHOWN IN FIG. 1

	Fig. 1(a)	Fig. 1(b)	
Methods	d(P,Q)	d(P,S)	Δ
$\|\|.\|\|_2$	1.764	0.963	0.801
EMdist	1.358	0.716	0.642
HD	2.184	0.403	1.781

measures between P and S. Hence, by analyzing the measures shown in Table I and without looking at Fig. 1, we find that the distances in Fig. 1(b) are almost 300 times bigger than those of Fig. 1(a) even though in terms of geometric distance, curves of Fig. 1(b) are closer than those in Fig. 1(a). Therefore, as opposed to the information-theoretic measures, more elaborate geometric measures should give us a better insight in this case.

C. Other Measures/Distances

We discuss in the following distances that will be more efficient for identifying the relevant modes of a signal.

1) $\ell 2$-norm: The $\ell 2$-norm corresponds to the standard usually used the distance between two points in a plane or in space. Hence, for two pdfs P and Q, the $\ell 2$-norm is defined by

$$||\mathrm{P}-\mathrm{Q}||_2 := \left(\int_{-\infty}^{+\infty} (\mathrm{P}(\mathrm{z})-\mathrm{Q}(\mathrm{z}))^2 \mathrm{dz}\right)^{\frac{1}{2}}. \quad (7)$$

A noteworthy feature of $\ell 2$-norm is that the contribution of a point is more important as its distance to the corresponding point increases. Hence, this measure can be useful for determining the geometric distance between densities.

2) Earth Mover's Distance: If two pdfs are normalized, the earth mover's distance (EMdist) is equivalent to the 1st Wasserstein distance, which is a natural way to compare the pdfs of two variables P and Q, where one variable is derived from the other by small, nonuniform perturbations [14]. Hence, by considering the fact that a number of IMFs will catch the clean signal, this distance can be efficient as selection criterion (SC) for the relevant modes. It is noteworthy that till now EMdist is essentially used in pattern recognition.

3) Hausdorff Distance: HD is a nonlinear operator, which measures the similarity between two sets or two geometric shapes. This distance has found the applications essentially in image processing. The HD between two point sets A and B is defined as follows:

$$\begin{aligned} \mathrm{HD}(\mathrm{A},\mathrm{B}) &= \max(\mathfrak{D}(A,B),\mathfrak{D}(B,A)) \\ \mathfrak{D}(\mathrm{A},\mathrm{B}) &= \max_{a\in A}\min_{b\in B}||a-b|| \\ \mathfrak{D}(\mathrm{B},\mathrm{A}) &= \max_{b\in B}\min_{a\in A}||b-a||. \end{aligned} \quad (8)$$

Two sets are close in HD if each point of either set is close to a given point of the other set. In this context, the most striking fact is that HD will be used as a similarity measure between two 1-D-signal pdfs, rather than between two geometric shapes. This distance shows how much IMF distribution curves are sharp and narrow [12].

Similarity measures HD, EMdist, and $\ell 2$-norm are applied to pdfs shown in Fig. 1. The best result is obtained using HD (Table II). However, the $\ell 2$-norm and the EMdist give close results as HD and compared with the results obtained if we use the information-theoretic measures, the three distances achieve the desired goal ($\Delta > 0$).

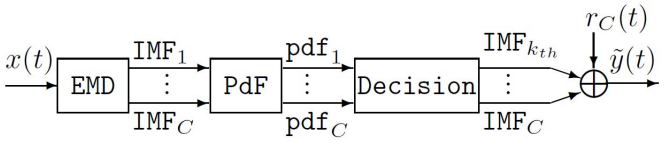

Fig. 2. Block diagram of the filtering method.

D. Identification of Relevant Modes

To identify the relevant modes, $x(t)$ is first decomposed into IMFs followed by an estimation of their pdfs (Fig. 2). The aim is to find the modes, which better represent $x(t)$ using only their pdfs and without any *a priori* knowledge about $y(t)$. The similarity measure, L, between the pdf of $x(t)$ and that of each IMF is defined as follows:

$$\mathrm{L}(i) = \mathrm{distance}[\mathrm{pdf}(x(t)), \mathrm{pdf}(\mathrm{IMF}_i(t))]. \quad (9)$$

The first selected mode is the one, for which the distance starts decreasing after the first local maximum. We note k_{th} the index of this mode identified by

$$k_{\mathrm{th}} = \arg\max_{1\le i\le C}\{L(i)\}+1. \quad (10)$$

E. Application

We show how to retrieve the relevant modes using their pdfs by $\ell 2$-norm, EMdist, HD, KLD, $\mathrm{KLD}_{\mathrm{sym}}$, and JSD measures on a signal $x(t)$ composed of two-tone signal and contaminated by a white Gaussian noise, $n(t)$, where the input signal-to-noise ratio ($\mathrm{SNR}_{\mathrm{in}}$) is fixed to 5 dB

$$x(t) = y(t)+n(t),\ y(t) = \cos(2\pi f_1 t)+\sin(2\pi f_2 t) \quad (11)$$

where $f_1 = 2$ Hz and $f_2 = 4$ Hz. Theoretically speaking, if f_1 and f_2 are known, the seventh and the eighth modes can be easily identified as the pure two tones. A careful examination of Fig. 3 shows that pdfs of these two modes are the closest to pdf of $x(t)$ compared with the other densities. The KLD, $\mathrm{KLD}_{\mathrm{sym}}$, and JSD measures fail to identify the relevant IMFs, resulting in an information-free signal [Fig. 4(a)]. Overall, they identify first to sixth IMFs (noisy modes) as the relevant modes. However, HD, EMdist and $\ell 2$-norm detect the relevant modes [Fig. 4(b)]. Thereafter, we will use these distances for filtering rather than the information-theoretic measures. The curves in Fig. 4(b) show the increase in HD, EMdist, and $\ell 2$-norm until the last noise-dominated mode (sixth IMF), then it decreases until it reaches its minimum at the IMF that best describes the noise-free signal $y(t)$ (seventh IMF). Thus, kth index is set to 7. The filtered signal shown in Fig. 5 shows the effectiveness of these measures. In some cases, the curves may increase again after the first local maximum, but this increase is because of the fact that the latter modes have very low amplitudes, and therefore their variances are small compared with the original signal [12].

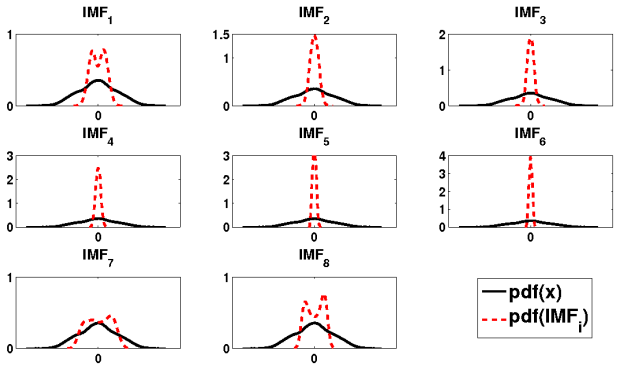

Fig. 3. Superposition of pdf of $x(t)$ and those of its modes.

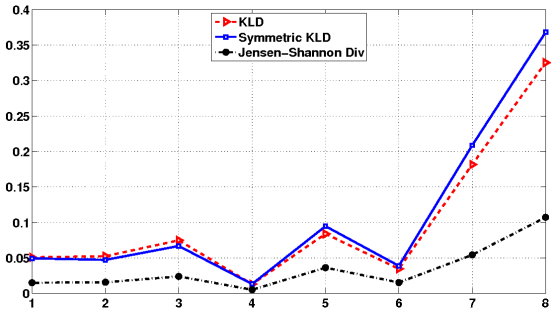

(a)

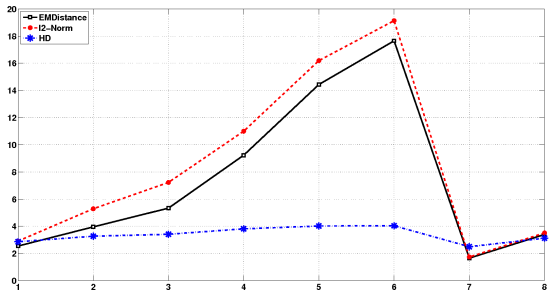

(b)

Fig. 4. (a) KLD, $\mathrm{KLD}_{\mathrm{sym}}$, and JSD versus IMF index of $x(t)$. (b) EMdist, HD, and $\ell 2$-norm versus IMF index of $x(t)$.

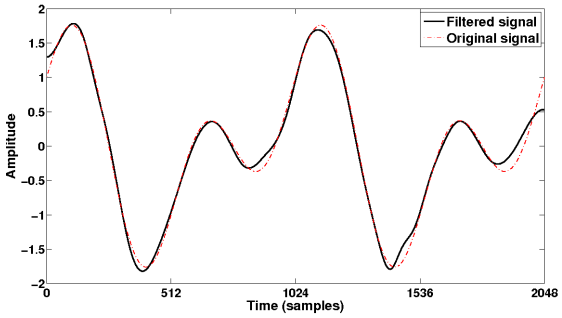

Fig. 5. Solid line: filtered signal. Dashed line: original signal.

III. Results and Discussions

We have conducted Monte Carlo (MC) simulations to assess the performance of the pdf-based filtering. We show the effectiveness of the filtering on both synthetic and real data. We compare the performances of white noise characteristics (WNC) and SC and CMSE [8] methods.

A. MC Simulations

The aim is to seek the optimal set of IMFs that yields the best partial reconstruction in terms of output SNR ($\mathrm{SNR}_{\mathrm{out}}$). We tackle this problem by evaluating exhaustively all possible combinations of modes to extract the optimal set of IMFs. It is simple to show that the total number of combinations of j modes from J_l^s extracted IMFs are given by

$$\mathrm{T}_l^s = \sum_{j=1}^{J_l^s} \binom{J_l^s}{j}. \tag{12}$$

J_l^s is the number of IMFs extracted in the s^{th} MC trial for $\mathrm{SNR}_{in}\delta l$dB where δ is step size of SNR and $l \in \mathbb{Z}$. For each trial and a combination of modes, the filtered signal $\tilde{y}(t)$ is reconstructed and the associated $\mathrm{SNR}_{\mathrm{out}}$, noted $\mathrm{SNR}_0(s,l)$, is calculated. For S trials, the total number of reconstructions is $T_r = S \times T_l^s$. We determine the optimal set of modes, for each SNR $= \delta l$ dB, as the one that yields the maximum of all the SNRs

$$\mathrm{SNR}_{\max}(l) = \max_{1 \le s \le T_r} \{\mathrm{SNR}_0(s,l)\}. \tag{13}$$

We compare, in terms of $\mathrm{SNR}_{\mathrm{out}}$, the filtered signal obtained by the optimal combination, noted R_0. The reconstructions yielded by $\ell 2$-norm, EMdist, and HD methods are designated, respectively, as R_1, R_2, and R_3. We include in this comparison, the SC proposed in [11], and WNC approach introduced in [9]. WNC and SC are noted, respectively, as methods R_4 and R_5. For each SNR value, δl, we evaluate the performance of each filtering R_i in terms of $\mathrm{SNR}_{\mathrm{out}}$ compared with method R_0 as follows:

$$\mathrm{pt}(s,l) = \begin{cases} 1/T_r, & \text{if } \mathrm{SNR}_{\max}(l) = \mathrm{SNR}_i(s,l),\ i \in \{1,2,\ldots 5\} \\ 0 \quad\ , & \text{otherwise} \end{cases}$$

where $\mathrm{SNR}_i(s,l)$ is the $\mathrm{SNR}_{\mathrm{out}}$ of the method R_i corresponding to $\mathrm{SNR}_{\mathrm{in}}$ δl and to trial s, $s \in \{1,2,\ldots,S\}$. Function $pt(s,l)$ designates the percentage of how much the method R_i gives the best result. We carried out the simulations with SNR values varying from -10 to 10 dB with $\delta = 2$ dB. We ran $S = 10\,000$ MC trials for each SNR value l where $l \in \{-5,-4,\ldots,5\}$. Only results of $l = -5,-2,2$, and 5 are presented. For illustrative purpose, if J_l^s is equal to eight IMFs the number of estimates per SNR value is 2.55 million. This number of estimates is necessary for statistical analysis because more trials are required, particularly, for lower SNR's. Results of comparison of the R_i methods shown in Table III show the superior performance of pdf-based filtering over the WNC and SC methods. Best results are given by $\ell 2$-norm. These results not only support the effectiveness of $\ell 2$-norm, EMdist, and HD as similarity measures but also mostly, show that the signal information's carried in the IMFs can be unveiled by their pdfs.

TABLE III

PERCENTAGE OF HOW MUCH THE METHOD R_i GIVES THE BEST RESULTS FOR $x(t)$

	Methods	-10dB	-4dB	4dB	10dB
R_1	EMD $-\ ||.||_2$	83.40%	87.10%	93.23%	94.40%
R_2	EMD-EMdist	82.38%	84.59%	86.24%	88.30%
R_3	EMD-HD	80.81%	83.12%	88.93%	89.60%
R_4	EMD-WNC	18.71%	81.92%	81.77%	60.42%
R_5	EMD-SC	58.64%	36.86%	11.67%	7.15%

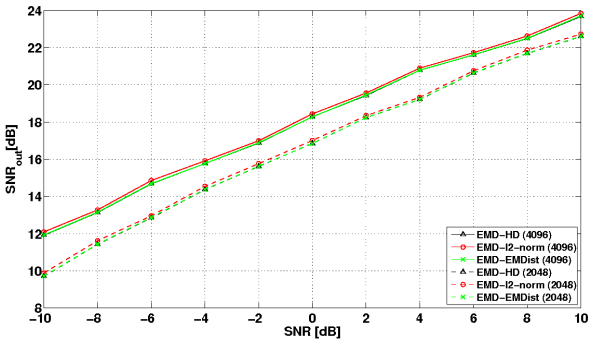

Fig. 6. Performance evaluation of EMD-based filtering techniques (HD, $l2-$ norm, and EMdist).

B. Synthetic Data

We illustrate the performances of the five methods on two representative test signals: Blocks and Heavysine, with SNR_{in} varying from -10 to 10 dB with $\delta = 2$ dB. We perform a MC simulation for each method, generating 50 realizations of the noise for each SNR_{in} value. We first compare the performances of the pdf-based filtering methods with $\text{SNR}_{\text{in}} =$ 5 dB. Fig. 6 shows this comparison on Heavysine signal of duration $D = 4$ s and sampled with two sampling frequency $f_{s1} = 512$ Hz (dashed line) and $f_{s2} = 2f_{s1}$ (solid line). As in Table III, HD, $\ell 2$-norm, and EMdist perform similarly. But $\ell 2$-norm shows slightly better SNR_{out} than HD and EMdist at all SNR_{in} levels. In addition, the pdf-based filtering improves significantly the SNR_{out}. The gain in SNR is up to 20 and 22 dB for f_{s1} and f_{s2}, respectively. This result is expected, since the sifting quality depends on the number of extrema, which in turn depends on the sampling frequency used. Fig. 6 also shows that increasing the sampling rate improves the SNR by 1.5 to 2.5 dB. Because the three methods perform similarly, which is consistent with findings shown in Table III, we henceforth limit the comparisons with $\ell 2$-norm. Figs. 7 and 8 show the comparison of WNC, CMSE, $\ell 2$-norm, and SC for the two signals and show the superiority of $\ell 2$-norm for all SNR_{in} levels over WNC, CMSE, and SC. For SNR ≥ 6 dB, the four methods have the same behavior but $\ell 2$-norm is still the best approach. For SNR ≤ -2 dB, the WNC method provides less good results than the other methods. Even if Blocks and Heavysine signals have different structures, from the results shown in Figs. 7 and 8, the same conclusions can be drawn in terms of performance. These results demonstrate that the pdf-based similarity is well suited for filtering a piecewise

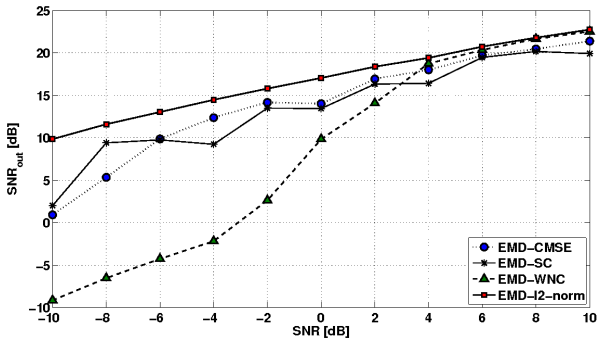

Fig. 7. SNR_{out} versus SNR_{in} for Heavysine signal.

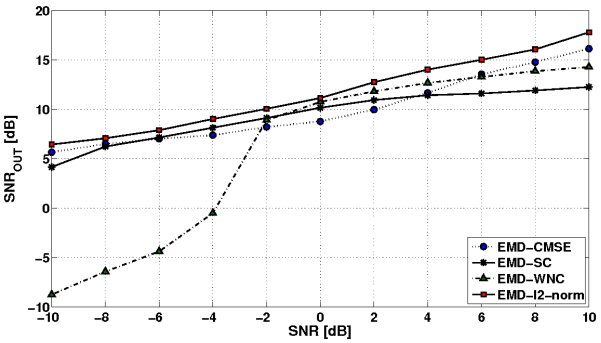

Fig. 8. SNR_{out} versus SNR_{in} for Blocks signal.

TABLE IV

MSE AND SNR_{out} VARIANCE COMPARISON FOR SIGNALS CORRUPTED WITH ADDITIVE WHITE GAUSSIAN NOISE (SNR = 5 dB)

Methods	Heavysine		Blocks	
	MSE	var(SNR)	MSE	var(SNR)
EMD-WNC	9.52	36.862	0.278	0.660
EMD-SC	4.98×10^{-2}	14.011	0.290	4.790
EMD-CMSE	1.96×10^{-1}	16.290	0.230	5.990
EMD $-\ ||.||_2$	$\mathbf{3.05 \times 10^{-2}}$	**0.718**	**0.137**	**0.513**

constant with jumps signals (Blocks) or oscillating ones (like Heavysine). In addition to SNR_{out} values, the performances are compared in terms of MSE calculated between the filtered and the original signals. Another measure that characterizes the filtering performance is the variance of the SNR_{out} estimates, resulting from different realizations, which is an indicator of robustness of the method. We perform a MC simulation using 50 trials to determine the MSE of the reconstructed signals for $\text{SNR}_{\text{in}} = 3$ dB and estimate the corresponding variances. Results shown in Table IV show that $\ell 2$-norm provides the lowest reconstruction error and variance for both signals showing the robustness and the superiority of this method over WNC, SC, and CMSE approaches.

C. Biomedical Data

We first test the filtering on ECG signal. Fig. 9 shows the application of $\ell 2$-norm approach to $x(t)$ signal, and compared with a noise-free signal $y(t)$, the characteristic features of ECG are well preserved in the reconstructed signal, $\tilde{y}(t)$.

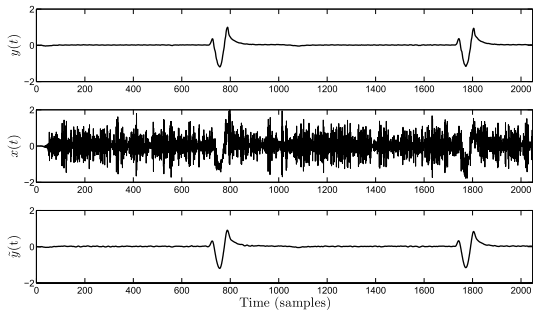

Fig. 9. Filtered ECG signal (bottom), noisy signal (middle), and original ECG (top).

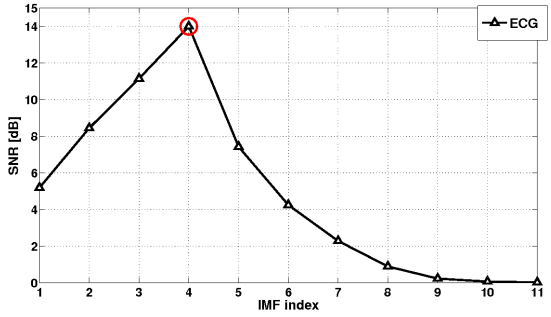

Fig. 10. SNR_{out} versus IMF index for ECG using $\ell 2$-norm (circle indicates the k_{th} value).

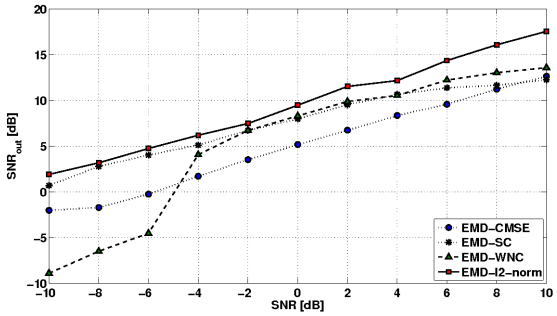

Fig. 11. SNR_{out} versus SNR_{in} for ECG signal.

TABLE V
MSE AND SNR_{out} VARIANCE COMPARISON FOR NOISED ECG SIGNAL

Methods	MSE	var(SNR)
EMD-WNC	4.24×10^{-2}	0.7839
EMD-SC	1.16×10^{-3}	2.9524
EMD-CMSE	3.86×10^{-1}	3.3530
$\text{EMD} - \|\|.\|\|_2$	$\mathbf{2.08 \times 10^{-4}}$	**0.3817**

Fig. 10 shows that $\ell 2$-norm method clearly identifies k_{th} value as the maximum of SNR_{out}, supporting the fact that the pdf of the modes captures the main structures of $y(t)$. As for synthetic signals (Figs. 7 and 8), results of Fig. 11 again show that $\ell 2$-norm outperforms WNC, SC, and CMSE methods. These results are confirmed by those shown in Table V particularly in terms of robustness.

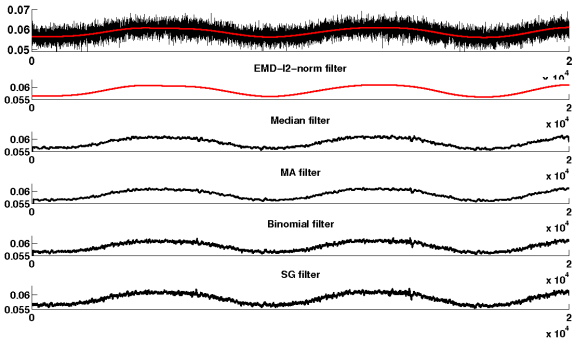

Fig. 12. Hydrodynamical measured and filtered signals.

D. Hydrodynamic Data

In the second experiment, filtering is tested on real hydrodynamical signal. This signal, contaminated by a colored noise, corresponds to a near-wall pressure signal of an hydrofoil's suction side undergoing a forced rotational motion while facing incoming flow in a hydrodynamic tunnel [15]. In a forced oscillatory motion, one looks at the first step to retrieve the component of mechanical forcing, which is a periodical oscillatory signal with a known frequency from the signal [15]. The residual signal would have rich physical content. Fig. 12 (top plot) shows a measured signal (noisy) of forced oscillatory motion. With a conventional bandpass filtering, one can retrieve the periodical oscillatory component but this supposes that filter parameters (central frequency of each filter, bandwidth,…) to be known beforehand. The extracted oscillatory component obtained by $\ell 2$-norm is superimposed on the original signal (Fig. 12). This result shows that this component is well extracted without any *a priori* knowledge about the input signal. More precisely, it can be seen that the oscillatory component is very smooth and follows the underlying characteristics of the signal. For comparative purpose, we also plot the performance of conventional filtering methods: Savitzky–Golay (SG) filter, median filter, moving average filter, and Binomial filter. These methods retrieve the oscillatory component with noticeable ripples and fluctuations along the signal in time and particularly for SG filter (down plot). The results of these methods are conditioned by the setting of the length of the time window analysis. The $\ell 2$-norm filter outperforms these classical filters without using any thresholds or parameters.

E. Aerodynamic Data

In the previous experiments, the signals are severely contaminated by noise. In the third experiment we show that, even in moderate noise contamination, the proposed approach works well and does not induce an over-filtering of the signal. Indeed, conventional filtering will not suppress unwanted noise but also some structures of the signal. The data are recorded on an instrumented yacht sailing upwind in a moderate head swell [16]. The wind signal is recorded at the top mast by an acoustic anemometer giving the instantaneous apparent wind angle $\text{AWA}_{\dot{\theta}}(t)$ and apparent wind speed $\text{AWS}_{\dot{\theta}}(t)$. The boat attitude in pitching $\dot{\theta}(t)$ is recorded by a central

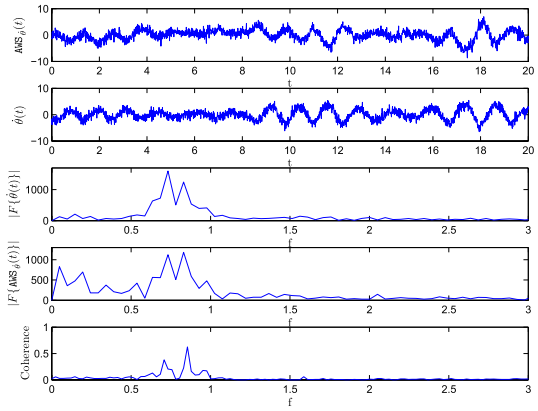

Fig. 13. Analysis of noisy AWS signal.

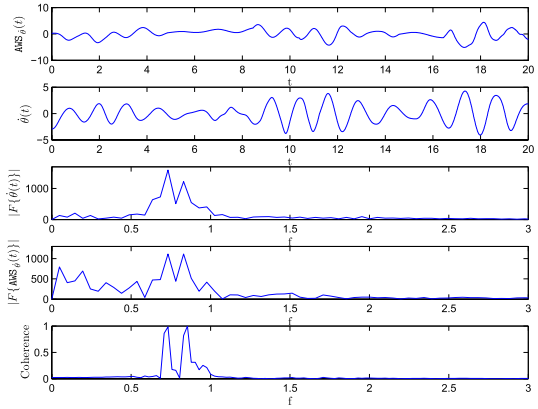

Fig. 14. Analysis of filtered AWS signal.

of attitude placed at the center of rotation of the hull. The pitching motion due to head swell affects the apparent wind by adding a pitching-induced velocity along the mast. Signal $\mathrm{AWS}_{\dot{\theta}}(t)$ is linked to an apparent wind speed AWS(t) and angle AWA(t) without pitching motion [16]. Variations of $\mathrm{AWS}_{\dot{\theta}}(t)$ linked to the frequency of wave encounter are the reason for the aerodynamic performance oscillation of the sail plan when pitching [16]. In the 20-s record, the swell has two different periods, consequences for two frequencies of wave encounter $f_1 = 0.73$ Hz and $f_2 = 0.85$ Hz. Noisy versions of $\mathrm{AWS}_{\dot{\theta}}(t)$ and $\dot{\theta}(t)$ signals are shown in Fig. 13. Fig. 14 shows that $\ell 2$-norm filtering preserves the structures of the signals very well. In addition, spectral analysis shows that the frequency contents of this signal are slightly affected by the filtering (Figs. 13 and 14) where $|F\{h(t)\}|$ is the amplitude spectrum of signal $h(t)$. More particularly, the frequencies f_1 and f_2 of wave encounter are revealed very clearly in the filtered signals, illustrating the adaptive nature of EMD combined with pdf-based measure. These frequencies, present in $\mathrm{AWS}_{\dot{\theta}}(t)$ and $\dot{\theta}(t)$, are more strongly evidenced by the coherence function as common frequencies in filtered case (Fig. 14) than in noisy case (Fig. 13). These results show that over-filtering, which can occur in a conventional filtering can be avoided using the pdf-based filtering approach. Same conclusions can be done on the analysis of $\mathrm{AWA}_{\dot{\theta}}(t)$ and $\dot{\theta}(t)$ signals.

IV. Conclusion

In this paper, a new adaptive filtering strategy is presented. The filtering makes use of partial reconstruction, the relevant modes being selected on the basis of probabilistic similarity measure between the pdf of the input signal and that of each extracted mode. This filtering exhibits an enhanced performance compared with the classical filters and to EMD-based filtering strategies reported in the literature. The best results are given by the geometric similarity measures (especially the $\ell 2$-norm) who proved to be more efficient than the information-theoretic measures. In addition, the results show that the signal information carried in the IMFs are unveiled by their pdfs. In addition, the pdf similarity measure proved to be more robust than the correlation, which is a very noise-sensitive measure, one of the advantages of which is its low complexity making it very practical for filtering applications. To confirm the obtained results and the effectiveness of the approach, the filtering strategy must be evaluated with a large class of real signals and in different experimental conditions such as varying sampling rates or other types of noise.

References

[1] Y. W. Tang, C. C. Tai, C. C. Su, C. Y. Chen, and J. F. Chen, "A correlated empirical mode decomposition method for partial discharge signal denoising," *Meas. Sci. Technol.*, vol. 21, no. 8, p. 085106, 2010.

[2] M. D. Kusljevic, J. J. Tomic, and L. D. Jovanovic, "Frequency estimation of three-phase power system using weighted-least-square algorithm and adaptive FIR filtering," *IEEE Trans. Instrum. Meas.*, vol. 52, no. 2, pp. 322–329, Feb. 2010.

[3] D. Dey, B. Chatterjee, S. Chakravorti, and S. Munshi, "Importance of denoising in dielectric response measurements of transformer insulation: An uncertainty analysis based approach," *Measurement*, vol. 43, no. 1, pp. 54–66, 2010.

[4] L. Xu and Y. Yan, "An improved algorithm for the measurement of flame oscillation frequency," *IEEE Trans. Instrum. Meas.*, vol. 56, no. 5, pp. 2087–2093, Oct. 2007.

[5] A. Ferrero and S. Salicone, "Measurement uncertainty," *IEEE Trans. Instrum. Meas.*, vol. 9, no. 3, pp. 44–51, Jan. 2006.

[6] D. Donoho, "De-noising by soft-thresholding," *IEEE Trans. Inform. Theory*, vol. 41, no. 3, pp. 613–627, May 1995.

[7] N. E. Huang, Z. Shen, S. R. Long, M. C. Wu, H. H. Shih, Q. Zheng, N. C. Yen, C. C. Tung, and H. H. Liu, "The empirical mode decomposition and the Hilbert spectrum for nonlinear and non-stationary time series analysis," *Proc. R. Soc. London*, vol. 454, pp. 903–995, Mar. 1998.

[8] A. O. Boudraa and J. C. Cexus, "EMD-based signal filtering," *IEEE Trans. Instrum. Meas.*, vol. 56, no. 6, pp. 2196–2202, Dec. 2007.

[9] Z. Wu and N. E. Huang, "A study of the characteristics of white noise using the empirical mode decomposition method," *Proc. R. Soc. London, A*, vol. 460, no. 2046, pp. 1597–1611, 2004.

[10] Z. K. Peng, W. T. Peter, and F. L. Chu, "Comparison study of improved Hilbert-Huang transform and wavelet transform: Application to fault diagnosis for rolling bearing," *Mech. Syst. Signal Proc.*, vol. 19, no. 5, pp. 974–988, 2005.

[11] X. Ayenu-Prah and N. O. Attoh-Okine, "A criterion for selecting relevant intrinsic mode functions in empirical mode decomposition," *Adv. Adapt. Data Anal.*, vol. 2, no. 1, pp. 1–24, 2010.

[12] A. Komaty, A. O. Boudraa, and D. Dare, "EMD-based filtering using the Hausdorff distance," in *Proc. IEEE ISSPIT*, Feb. 2012, pp. 1–12.

[13] T. M. Cover and J. A. Thomas, *Elements of Information Theory*. New York, NY, USA: Wiley, 2006.

[14] O. Pele and M. Werman, "Fast and robust earth mover's distances," in *Proc. Int. Conf. Comput. Vis.,* 2009, pp. 460–467.

[15] S. Benramdane, J. A. Astolfi, J. C. Cexus, and A. O. Boudraa, "Experimental investigation of wall-pressure fluctuations on a transiently moving hydrofoil by empirical mode decomposition," in *Proc. ISOPE Conf.*, 2007, pp. 1–7.

[16] B. Augier, P. Bot, F. Hauville, and M. Durand, "Experimental validation of unsteady models for fluid structure interaction: Application to yacht sails and rigs," *J. Wind Eng. Indus. Aerodyn*, vol. 101, no. 14, pp. 53–66, 2012.

Ali Komaty (S'12) received the B.E.E. degree from Lebanese University, Beirut, Lebanon, in 2009, and the M.S. degree from Ecole Nationale d'Ingénieurs de Brest, Brest, France, in 2010. He is currently pursuing the Ph.D. degree in Underwater Acoustics Group with the French Naval Academy Research Institute, Brest.

His current research interests include signal processing, empirical mode decomposition, time-frequency analysis, and blind source separation.

Abdel-Ouahab Boudraa (SM'06) was born in Constantine, Algeria. He received the B.S. degree in physics (electronics engineering) from the Constantine Institute of Physics, University of Constantine, Constantine, and the Engineer degree in electronics from Educatel, Liege, Belgium, the M.Sc. degree in biomedical engineering from INSA, Lyon, University degree in nuclear magnetic resonance, and the Ph.D. degree in image processing and the University degrees in statistics and modeling and in positron emission tomography from the University of Claude Bernard, Lyon 1, France.

He is currently an Associate Professor of electrical engineering with Ecole Navale, Brest, France. His current research interests include computer vision, vector quantization, data structures and analysis, data fusion, time-frequency analysis, higher-order energy operators, empirical mode decomposition, and hard and fuzzy pattern recognition.

Dr. Boudraa was a recipient of the 2003 Varian Prize Award by the Swiss Society of Radiobiology and Medical Physics for the Best Published Paper impacting Radiation Oncology.

Benoit Augier received the Degree in naval architecture from Danish Technical University, Copenhagen, Denmark, the M.Sc. degree in engineering from ENSAM ParisTech, Paris, France, in 2008, and the Ph.D. degree in mechanics and energy from the Naval Environment Department, French Naval Academy Research Institute, Brest, France, in 2012.

He is currently a Post-Doctoral Fellow with the Department of Structural Engineering, University of California, San Diego, CA, USA. His current research interests include fluid structure interaction, dynamic behavior of a soft membrane, full scale experiment, signal processing, and computational fluid dynamics simulations.

Delphine Daré-Emzivat received the Ph.D. degree in electronic and industrial control from the University of Bretagne Sud, Bretagne Sud, France.

She has been an Assistant Professor of signal processing with Ecole Navale, Brest, France, since September 2001. Her current research interests include beam forming and array processing techniques, time-frequency analysis, and detection and localization of buried objects.